Hindawi Publishing Corporation
Journal of Nanomaterials
Volume 2016, Article ID 3693249, 7 pages
http://dx.doi.org/10.1155/2016/3693249

Hindawi

Research Article

Experimental Research on Heat Transfer Characteristics of CuO Nanofluid in Adiabatic Condition

Yu Guangbin,[1] Gao Dejun,[1] Chen Juhui,[1] Dai Bing,[1] Liu Di,[1] Song Ye,[1] and Chen Xi[2]

[1]*School of Mechanical and Power Engineering, Harbin University of Science and Technology, Harbin, Heilongjiang 150080, China*
[2]*School of Mechanical Engineering, The University of Melbourne, Melbourne, VIC 3010, Australia*

Correspondence should be addressed to Chen Juhui; chenjuhui@hit.edu.cn

Received 17 August 2015; Revised 23 November 2015; Accepted 28 December 2015

Academic Editor: Nageh K. Allam

The laminar convective heat transfer behavior of CuO nanoparticle dispersions in glycol with the average particle sizes (about 70 nm) was investigated experimentally in a flow loop with constant heat flux. To enhance heat exchange under high temperature condition and get the more accurate data, we try to improve the traditional experimental apparatus which is used to test nanofluid heat transfer characteristics. In the experiment five different nanoparticle concentrations (0.25%, 0.50%, 0.80%, 1.20%, and 1.50%) were investigated in a flow loop with constant heat flux. The experimental results show that the heat transfer coefficient of nanofluid becomes higher than that of pure fluid at the same Reynolds number and increased with the increasing of the mass fraction of CuO nanoparticles. Results also indicate that at very low volume concentrations nanofluid has no major impact on heat transfer parameters and the pressure of nanofluids increased by the mass fraction increase.

1. Introduction

With the development of industry, traditional heat transfer fluids such as oil, water, and ethylene glycol are hardly satisfying the requirement of modern industry, transportation, nuclear, electronic engineering, and so forth. Therefore, it has been proposed that millimeter- or micrometer-sized particles could be suspended in industrial heat transfer fluids to employ. However, it has a lot of disadvantages in heat transfer fluids containing suspended particles of micrometer and millimeter size like clogging in small passages and erosions of the components by abrasive reactions. As a new class of engineered fluid, nanofluids were the first pioneered by Choi and Eastman in 1995 [1]; it has been proposed that nanometer-sized particles could be suspended in industrial heat transfer fluids such as water, ethylene glycol, and oil to produce a new class of engineered fluids with high thermal conductivity. Because of the excellent thermal conductivity, nanofluid dispersions are important for a number of industrial sectors including transportation, power generation, micromanufacturing, and miniature devices [2, 3].

Nanofluids as a new class of heat transfer fluids have already been researched by many researchers in the past few years. Pak and Cho [4] investigated turbulent heat transfer characteristics of γ-Al_2O_3/water and TiO_2/water nanofluid in a circular pipe in 1998. The results indicated that when the volume fraction of nanoparticles was 3%, the heat transfer coefficient of nanofluids compared with pure water is reduced by 12%. Kole and Dey [5] investigated the automobile cooling liquid of Al_2O_3 nanofluids and got the curvilinear relationship between viscosity/temperature and nanoparticle volume fraction. Zyła and Cholewa [6, 7] did the research on the unexpected behavior of viscosity of glycol-based $MgAl_2O_4$ nanofluids and shown that nanofluids have been studied very intensively because they may find many applications in many fields including science, industry, and medicine. Recently, many researchers [8–10] constructed an apparatus to investigate on the pool boiling heat transfer convective heat and friction factor of nanofluid. In addition, there are some other researchers [11–14] that do lots of experiments to study the heat transfer characteristics of nanofluid and all of them get the conclusion that, comparing with base fluid, nanometer-sized particles which were suspended in the industrial heat transfer fluids have bright advantages in heat transfer. Although there are many researchers that have already focused on the study of nanofluids heat transfer characteristics in

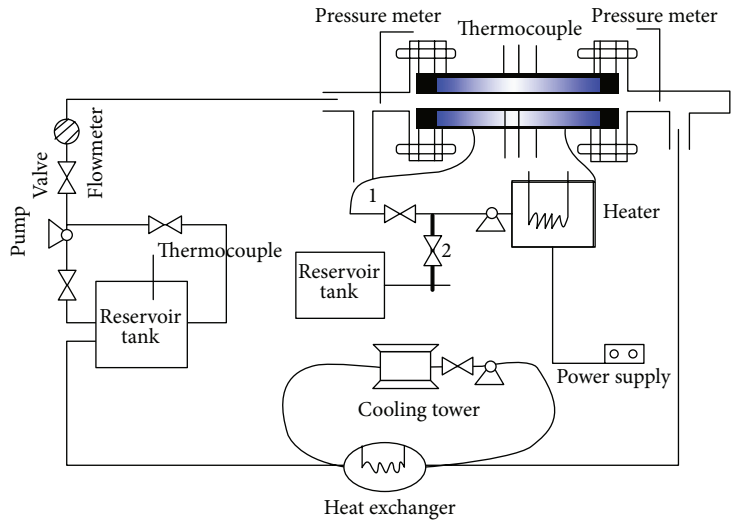

Figure 1: Schematic diagram of experimental apparatus.

copper tube, we had designed the experimental system; for example, the copper tube was heated by electric resistance wire but it could not heat uniformly and the data of experiment is not accurate.

This paper aims to consider effects of nanofluid coolant on heat transfer by improved setup and get the more accurate data. So it is better to understand the heat transfer characteristics of nanofluid compared with glycol fluid. Furthermore, the results from calculation of several Nusselt correlations were compared with the measured data. Because CuO nanofluids not only have high thermal conductivity but also make good compatibility with basic liquid, the cost is not too high. So taking the factors into consideration, CuO nanofluids will be selected.

Firstly, the theory of experiment and data parameter is discussed in Section 2. Secondly Section 3 provides the detailed theory of conducted heat. Thirdly, in Section 4, the relationship between Reynolds number and heat transfer coefficient (including pressure and flow) would be introduced. Finally some concluding remarks are made in Section 5.

2. The Building of Experimental System

2.1. Schematic Diagram of Experimental Setup. As is shown in Figure 1, the reservoir tank (about 5 liters) was made of polymethylmethacrylate and intended to hold the preparation of nanofluid, while being equipped with the thermocouple of the accuracy of 0.1°C, and the pressure of intake/outtake was measured by the pressure meter. A flow meter recorded the nanofluids quantity of flow; the bypass line was used to discharge liquid. The copper tube with an inner diameter of 25 mm and an external diameter of 30 mm and a length of 1000 mm was used as the test section; the copper tube casing was full of ethylene glycol. The tube surface was covered with heat preservation material of aluminum silicate and a fiber glass tape; the tube was fixed by flange plates on both ends and gauze with asbestos was located in the middle, which has the function of preserving heat.

There were two pyroelectric sensors (one has the accuracy of 0.1°C; another has the accuracy of 1°C) in the test section; they were used to measure the tube wall and fluid temperature. In order to control the fluid flow rate, a valve was used. The first circulatory system was made up of the reservoir tank and the test section; the system could measure the heat transfer coefficient of the nanofluid. Secondly circulatory system was a heat exchanger and a cooling tank; the function was to preserve constant temperature at the inlet of the test section. The third circulatory system was a heating device and a test section; the main function of that was to heat ethylene glycol which was located in the middle of the sleeve and the copper tube, to preserve a constant temperature of the tube wall.

2.2. The Experimental Step. In this section, the nanofluid with 50~60 nm CuO particles will be prepared different mass fractions for the experiment, and there are four steps that will be followed before analyzing the test data:

(1) Check out the air tightness of the test device.

(2) By making nanofluid with "two steps" and measuring little nanoparticles and dispersant, they were added into the glycol fluid and mixed in 120 minutes, making use of ultrasonic shaking in 150 minutes in order to get nanofluid suspension and we will use sodium dodecyl-benzenesulfonate (SDBS) as a dispersant. Furthermore, we observed the effect of nanofluid stability with different volume fraction of SDBS. In order to obtain stability nanofluid, we used sodium dodecylbenzenesulfonate (SDBS) as a dispersant. The volume of SDBS has a great impact on the stability of CuO-glycol nanofluid. By increasing the volume of SDBS, the stability of CuO-glycol is better.

(3) Measured nanofluid was added into the system; the export and import of the test section and the tube wall temperature were constant until making use of the heat device, heating copper tube equably.

(4) The heat sensor and thermocouple marked corresponding temperature; each measurement was repeated to measure different mass fraction nanofluid. Finally, we analyzed the measured data.

2.3. The Data of Convective Heat Transfer Analysis. In order to obtain heat transfer parameters, nanofluid properties such as density, specific heat, viscosity, and thermal conductivity should be measured or calculated by theoretical models.

Density and specific heat are given by Wang and Mujumdar [15]

$$\text{Density: } \rho_{\text{nf}} = (1-\varphi)\rho_{\text{bf}} + \varphi\rho_{\text{np}}. \tag{1}$$

Heat capacitance is as follows:

$$C_{p,\text{nf}} = \frac{(1-\varphi)\rho_{\text{bf}}C_{p,\text{bf}} + \varphi\rho_{\text{np}}C_{p,\text{np}}}{\rho_{\text{nf}}}. \tag{2}$$

Dynamic viscosity of nanofluid is as follows:

$$\mu_{\text{nf}} = (1 + 2.5\varphi)\mu_{\text{bf}}. \tag{3}$$

Reynolds number and thermal conductivity are given as follows.

The thermal conductivity of nanoparticles is given by Corcione [16]

$$\frac{k_{\text{nf}}}{k_{\text{bf}}} = 1 + 4.4R_{e\text{np}}^{0.4}P_{r\text{bf}}^{0.66}\left(\frac{T}{T_{fr}}\right)^{10}\left(\frac{k_{\text{np}}}{k_{\text{bf}}}\right)^{0.03}\varphi^{0.66}$$
$$P_{r_{\text{bf}}} = \frac{\mu_{\text{bf}}C_{p,\text{bf}}}{k}, \tag{4}$$

where T_{fr} is freezing point of base fluid (about 273.16 K).

Reynolds number is given as follows:

$$\text{Re}_{\text{np}} = \frac{\rho_{\text{bf}}Vd_{\text{np}}}{\mu_{\text{bf}}} = \frac{2\rho_{\text{bf}}\kappa_B T}{\pi\mu_{\text{bf}}^2 d_{\text{np}}}, \tag{5}$$

where κ_B is Boltzmann's constant (1.38066×10^{-23} J/K). This correlation is applicable for nanoparticles diameter between 10 nm and 150 nm, volume concentration between 0.2% and 9%, and nanofluid temperature between 294 K and 324 K.

3. The Theory of Conducted Heat

3.1. Parameter Calculation. With the convective heat transfer between nanofluid and copper tube wall, the temperature of nanofluid has changed on the inlet of the copper tube and outlet of the copper tube. Consider

$$\begin{aligned}
\dot{q} &= qC_{p,\text{nf}}\Delta T,\\
\Delta T &= T_{\text{out}} - T_{\text{in}},\\
q &= S\cdot v\cdot \rho_{\text{nf}},\\
S &= \frac{\pi {d_h}^2}{4},\\
v &= \frac{q_v}{s},
\end{aligned} \tag{6}$$

where $\dot{q}$ is generated heat, where $C_{p,\text{nf}}$ is the nanofluid specific heat and ΔT is the temperature difference of inlet copper and outlet copper. q is the average nanofluid mass flow, S is cross-sectional area of copper tube, v is the average velocity of nanofluid in the test section, and q_v is the average volume flow.

The nanofluid convective heat transfer coefficient $\overline{h}$ and Nu are calculated as follows [17] (which was given by Incropera and DeWitt):

$$\begin{aligned}
\overline{h} &= \frac{q''}{\overline{T_{\text{w}}} - \overline{T_{\text{f}}}},\\
q'' &= \frac{\dot{q}}{\dot{S}},\\
\text{Nu} &= \frac{hl}{k_{\text{nf}}},
\end{aligned} \tag{7}$$

where $\dot{S}$ is the surface area of test copper tube, $\dot{S} = \pi d \cdot L$, $\overline{T_{\text{w}}}$ is the average temperature of copper tube wall, and $\overline{T_{\text{f}}}$ is the average temperature of nanofluid. Consider

$$\begin{aligned}
\overline{T_{\text{w}}} &= \sum_{i=1}^{3}\frac{T_i}{3},\\
\overline{T_{\text{f}}} &= \frac{(T_{\text{out}} + T_{\text{in}})}{2}.
\end{aligned} \tag{8}$$

The arbitrary x heat transfer coefficient in the test section $h(x)$ is calculated as follows:

$$h(x) = \frac{q''}{T_{\text{w}}(x) - T_{\text{f}}(x)}, \tag{9}$$

where $T_{\text{w}}(x)$ is the arbitrary x of copper tube wall temperature and $T_{\text{f}}(x)$ is the arbitrary x temperature of nanofluid. Consider

$$T_{\text{f}}(x) = T_{\text{in}} + \frac{q''}{\rho_{\text{nf}}C_{p,\text{nf}}vSl}. \tag{10}$$

3.2. Uncertainty. The uncertainty of averaged heat transfer coefficient is defined as follows:

$$\delta R = \left\{\sum_{i=1}^{N}\left(\frac{\partial R}{\partial x_i}\delta x_i\right)^2\right\}^{1/2}. \tag{11}$$

The values of uncertainties were calculated in different Reynolds numbers and nanoparticles volume fractions. According to formula (11), we can get the uncertainties as Table 1.

4. Experimental Results and Discussion

4.1. The Effect of Nanofluid Stability with Different Volume Fraction of Dispersant. Figure 2 shows the typical micrographs obtained by transmission electron microscopy (TEM) for the CuO nanoparticles that were used in this study. Figure 2 confirms that the average size is 70 nm.

Table 1: The uncertainties.

Parameter	Uncertainty
Thermocouple	±5.1%
Pyroelectric sensor	±0.5%
Quantity of flow	±2.7%
Pressure	±4.5%
Transfer coefficient	±7.6%
Test section	±4.2%

4.2. Reynolds Number, Mass Fraction, and Heat Transfer Coefficient. A typical set of results are shown in Figure 3 for measurements at 20°C. The effective thermal conductivity of the nanofluid increases approximately linearly with particle volume fraction but decreases with increasing particle sizes [18, 19]. By the reason of the fact that nanoparticles size is big, the nanofluid thermal conductivity is not obvious at 0.50%. To obtain a comprehensive understanding of the mechanism behind this phenomenon, we also tested the samples with higher CuO concentration, and its heat transfer mechanism is similar to concentration at 1.20% (as the result is similar in the following Figures 4, 5, and 6, we did not introduce it). As is shown in Figure 3, for low volume of CuO nanoparticles in glycol fluid, there are no major changes in heat transfer coefficient. As the volume of CuO nanoparticles and the Reynolds number are increasing, however, the heat transfer coefficient of nanofluid has an obvious increase.

To obtain more data of experiment, we also measure the arbitrary of heat transfer coefficient in copper tube which is illustrated in Figure 4 at the temperature of 20°C.

As is shown in Figure 4 the heat transfer coefficient of entrance has an obvious difference in other places. The major reason is that it has a fierce Brownian movement in entrance [20, 21].

4.3. Reynolds Number, Mass Fraction, and Wall Temperature. In the third closed-loop system, shutdown valve 1 and open valve 2 lead ethylene glycol flow into the water tank, as shown in Figure 5.

Although there is no major effect on wall temperature in low nanoparticle concentrations, in higher volume fractions nanoparticles affect wall temperature. By increasing nanoparticle concentrations, wall temperature decreases. The reason behind this behavior is higher thermal conductivity of nanofluid in comparison to glycol fluid.

4.4. The Nusselt Number of Nanofluid in Different Nanoparticle Concentrations and Different Reynolds Number. Variation of Nusselt number with different particle concentrations at Re = 2600 is illustrated in Figure 6. It is evident that CuO nanoparticles suspended in ethylene glycol enhance the Nusselt number, except for 0.25% and 0.5% volume fractions.

4.5. The Resistance along the Project. The resistance along the project was reflected by the pressure variation with nanofluids

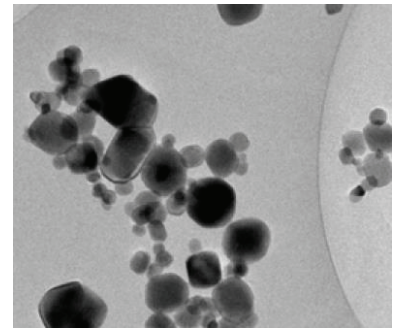

Figure 2: Typical TEM micrographs of CuO nanoparticles.

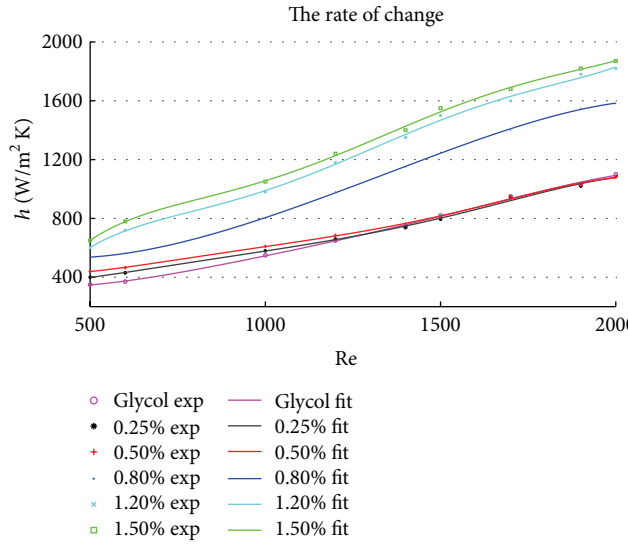

Figure 3: Convective heat transfer coefficient of CuO/glycol nanofluids with different mass fraction under laminar flow.

which was shown in Figure 6. And the relationship pressure with resistance is

$$f = \frac{2\Delta P d_h}{l \rho_{nf} v}, \tag{12}$$

where f is the resistance along the project, ΔP is the pressure drop of CuO-glycol, d_h is the hydraulic diameter, l is test section length, and v is velocity of flow.

In Figure 7, the pressure of nanofluids increased by the mass fraction increase. The major reason is that the higher particle volume fraction has a higher viscosity and its friction coefficient is also higher than the low particle volume fraction nanofluids. At the concentration of the CuO-glycol nanofluid from 0.80% to 1.20%, although its pressure is higher than others, the differential pressure is not very obvious. However, in the heat transfer aspect, the higher particle volume fraction nanofluid has a large obvious difference with the low ones. Although the pressure drop increases would lead to the loss of pimp power, the heat transfer coefficient increases significantly. That is to say, its thermal conductivity is higher than the low ones. So when the range of the CuO-glycol nanofluid

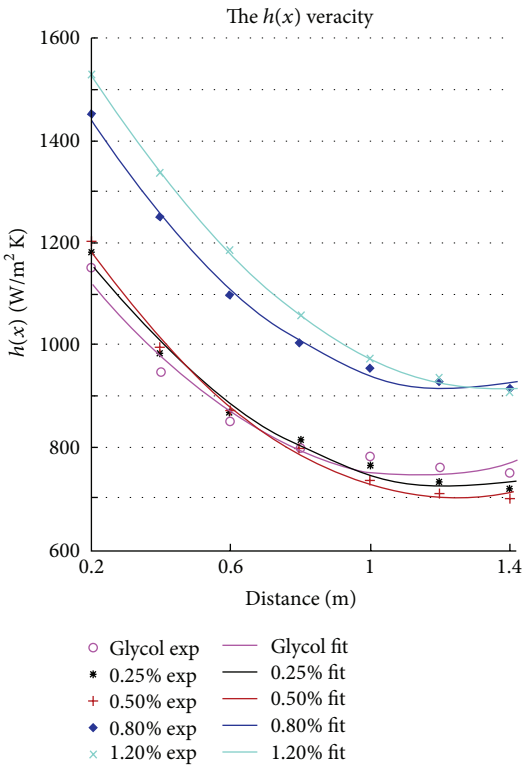

Figure 4: Tube axial convective heat transfer coefficient of CuO/glycol nanofluids with different mass fractions.

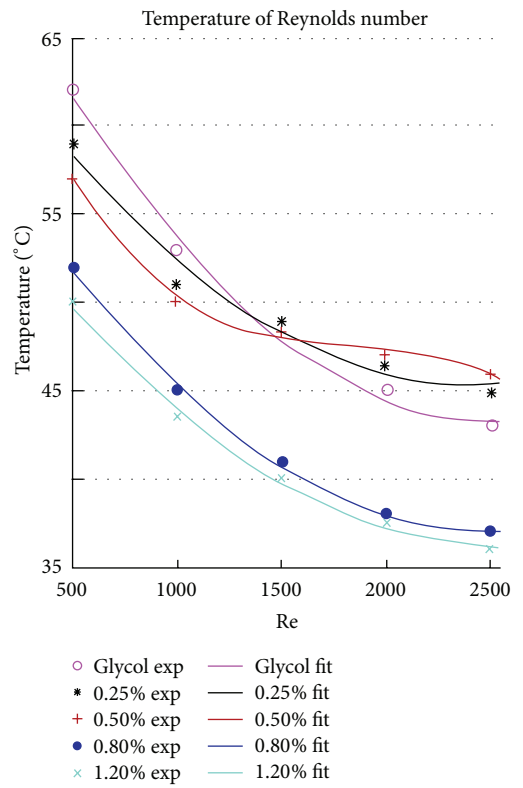

Figure 5: Measure the wall temperature.

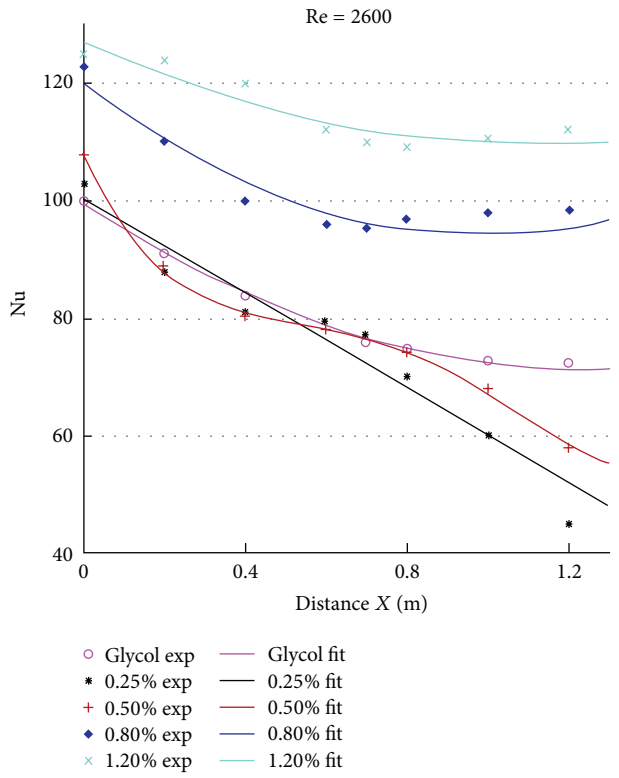

Figure 6: Tube axial local Nusselt number coefficient of CuO/glycol nanofluids with different mass fractions.

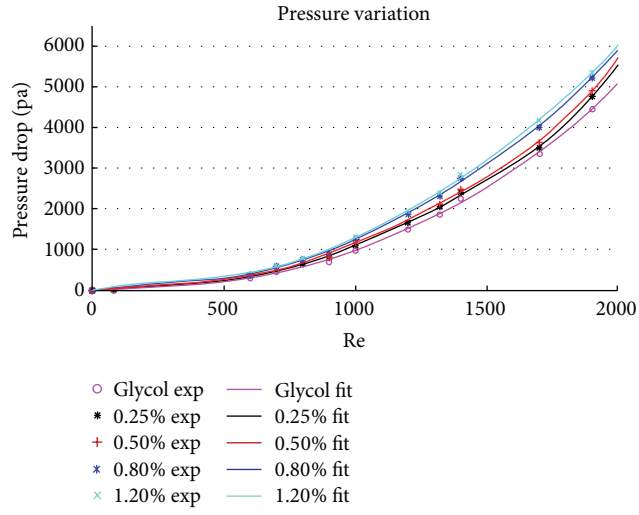

Figure 7: Pressure drop of CuO-glycol.

concentration is from 0.80% to 1.20%, its positive effects are much higher than negative effects.

5. Conclusions

(1) CuO nanoparticles make the heat transfer intensity of the fluid increase obviously in glycol fluid. It is observed that, by increasing Reynolds number, the heat transfer coefficient

increases, especially the inlet which is very obvious. Adding moderate dispersant can ease nanoparticles aggregation effectively and enable it to be steady.

(2) For higher volume fractions of CuO nanoparticle, wall temperature decreases and heat transfer increases.

(3) For low concentration of CuO nanofluid, there is no significant change in wall temperature, heat transfer coefficient, and Nusselt number. By increasing the mass fraction of CuO nanofluids, wall temperature decreases and heat transfer coefficient and Nusselt number increase.

(4) As nanofluids greatly increase the heat transfer coefficient of base liquid, compared to the defect taken by the volume of nanoparticle, its high heat transfer coefficient would bring more advantages. So increasing appropriately the particle volume fraction would be beneficial to the enhancement of heat transfer.

Nomenclature

C_p: Specific heat (J/kg)
D: Diameter of particles (nm)
d_h: Hydraulic diameter (mm)
Nu: Nusselt number
Pr: Prandtl number
$\dot{q}$: Generated heat (W)
Re: Reynolds number
κ: Boltzmann constant (J/K)
μ: Viscosity (kg/s m)
φ: Nanoparticles concentration
v: Velocity of flow (m)
bf: Base fluid
np: Nanoparticles
h: Heat transfer coefficient (W/m^2)
k: Thermal conductivity (W/m)
l: Test section length (mm)
p: Power (W)
q'': Heat flux (W/m^2)
d_{in}: Inner diameter (mm)
T: Temperature ($^\circ$C)
ρ: Density (kg/m^3)
q_v: Average volume flow
L: Test section length (mm).

Conflict of Interests

The authors declare that there is no conflict of interests regarding the publication of this paper.

Authors' Contribution

Chen Juhui and Yu Guangbin contributed equally to this work.

Acknowledgments

This research was supported by the National Natural Science Foundation of China (51406045) and the Key Program of National Natural Science Foundation of Heilongjiang (no. ZD201309), and the project was supported by the Major International Joint Research Program of China (Grant no. 2014DFB70120), the Outstanding Youth Science Fund of Heilongjiang (Grant no. JC201420) and National Natural Science Foundation of Heilongjiang Province (E201441).

References

[1] S. U. S. Choi and J. A. Eastman, "Enhancing thermal conductivity of fluids with nanoparticles," in *Proceedings of the International Mechanical Engineering Congress and Exhibition*, pp. 99–103, San Francisco, Calif, USA, November 1995.

[2] P. Garg, J. L. Alvarado, C. Marsh, T. A. Carlson, D. A. Kessler, and K. Annamalai, "An experimental study on the effect of ultrasonication on viscosity and heat transfer performance of multi-wall carbon nanotube-based aqueous nanofluids," *International Journal of Heat and Mass Transfer*, vol. 52, no. 21-22, pp. 5090–5101, 2009.

[3] B. Rimbault, C. T. Nguyen, and N. Galanis, "Experimental investigation of CuO-water nanofluid flow and heat transfer inside a microchannel heat sink," *International Journal of Thermal Sciences*, vol. 84, pp. 275–292, 2014.

[4] B. C. Pak and Y. I. Cho, "Hydrodynamic and heat transfer study of dispersed fluids with submicron metallic oxide particles," *Experimental Heat Transfer*, vol. 11, no. 2, pp. 151–170, 1998.

[5] M. Kole and T. K. Dey, "Viscosity of alumina nanoparticles dispersed in car engine coolant," *Experimental Thermal and Fluid Science*, vol. 34, no. 6, pp. 677–683, 2010.

[6] G. Zyła, M. Cholewa, and A. Witek, "Rheological properties of diethylene glycol-based $MgAl_2O_4$ nanofluids," *RSC Advances*, vol. 3, no. 18, pp. 6429–6434, 2013.

[7] G. Zyła and M. Cholewa, "On unexpected behavior of viscosity of diethylene glycol-based $MgAl_2O_4$ nanofluids," *RSC Advances*, vol. 4, no. 50, pp. 26057–26062, 2014.

[8] T. I. Kim, Y. H. Jeong, and S. H. Chang, "An experimental study on CHF enhancement in flow boiling using Al_2O_3 nano-fluid," *International Journal of Heat and Mass Transfer*, vol. 53, no. 5-6, pp. 1015–1022, 2010.

[9] M. Kole and T. K. Dey, "Investigations on the pool boiling heat transfer and critical heat flux of ZnO-ethylene glycol nanofluids," *Applied Thermal Engineering*, vol. 37, pp. 112–119, 2012.

[10] H. Ramakrishna, R. Shrikantha, and R. Ranapratap, "Experimental investigations of pool boiling heat transfer characteristics on a vertical surface using CuO nanoparticles in distilled water," *Heat Transfer Engineering*, vol. 35, no. 14-15, pp. 1279–1287, 2014.

[11] Y. Abbassi, M. Talebi, A. S. Shirani, and J. Khorsandi, "Experimental investigation of TiO_2/Water nanofluid effects on heat transfer characteristics of a vertical annulus with non-uniform heat flux in non-radiation environment," *Annals of Nuclear Energy*, vol. 69, pp. 7–13, 2014.

[12] V. T. Perarasu, M. Arivazhagan, and P. Sivashanmugam, "Heat transfer of TiO_2/water nanofluid in a coiled agitated vessel with propeller," *Journal of Hydrodynamics*, vol. 24, no. 6, pp. 942–950, 2012.

[13] C. T. Nguyen, N. Galanis, G. Polidori, S. Fohanno, C. V. Popa, and A. Le Bechec, "An experimental study of a confined and submerged impinging jet heat transfer using Al_2O_3-water nanofluid," *International Journal of Thermal Sciences*, vol. 48, no. 2, pp. 401–411, 2009.

[14] S. Mitra, S. K. Saha, S. Chakraborty, and S. Das, "Study on boiling heat transfer of water-TiO_2 and water-MWCNT nanofluids based laminar jet impingement on heated steel surface," *Applied Thermal Engineering*, vol. 37, pp. 353–359, 2012.

[15] X.-Q. Wang and A. S. Mujumdar, "Heat transfer characteristics of nanofluids: a review," *International Journal of Thermal Sciences*, vol. 46, no. 1, pp. 1–19, 2007.

[16] M. Corcione, "Empirical correlating equations for predicting the effective thermal conductivity and dynamic viscosity of nanofluids," *Energy Conversion and Management*, vol. 52, no. 1, pp. 789–793, 2011.

[17] K. Seung-Won, J. Jae-Jun, and L. Tae-Hee, "Candidate points and representative cross-validation approach for sequential sampling," *Korea Science*, vol. 44, pp. 367–373, 1996.

[18] S. Lee, S. U.-S. Choi, S. Li, and J. A. Eastman, "Measuring thermal conductivity of fluids containing oxide nanoparticles," *ASME Journal of Heat Transfer*, vol. 121, no. 2, pp. 280–288, 1999.

[19] H. Xie, J. Wang, and T. Xi, "Thermal conductivity enhancement of suspension containing nanosized alumiua particles," *Journal of Applied Physics*, vol. 97, no. 7, pp. 4568–4572, 2002.

[20] Y. Xuan and Q. Li, "Experimental investigation on heat transfer enhancement of nanofluids," in *Proceedings of the International Symposium on Nano-Materials and Technology*, Beijing, China, 2001.

[21] Q. Li and Y. Xuan, "Convective heat transfer performances of nanofluids," in *Proceedings of the 12th International Heat Transfer Conference*, Grenoble, France, August 2002.